Figures and figure supplements

Evolution of alternative biosynthetic pathways for vitamin C following plastid acquisition in photosynthetic eukaryotes
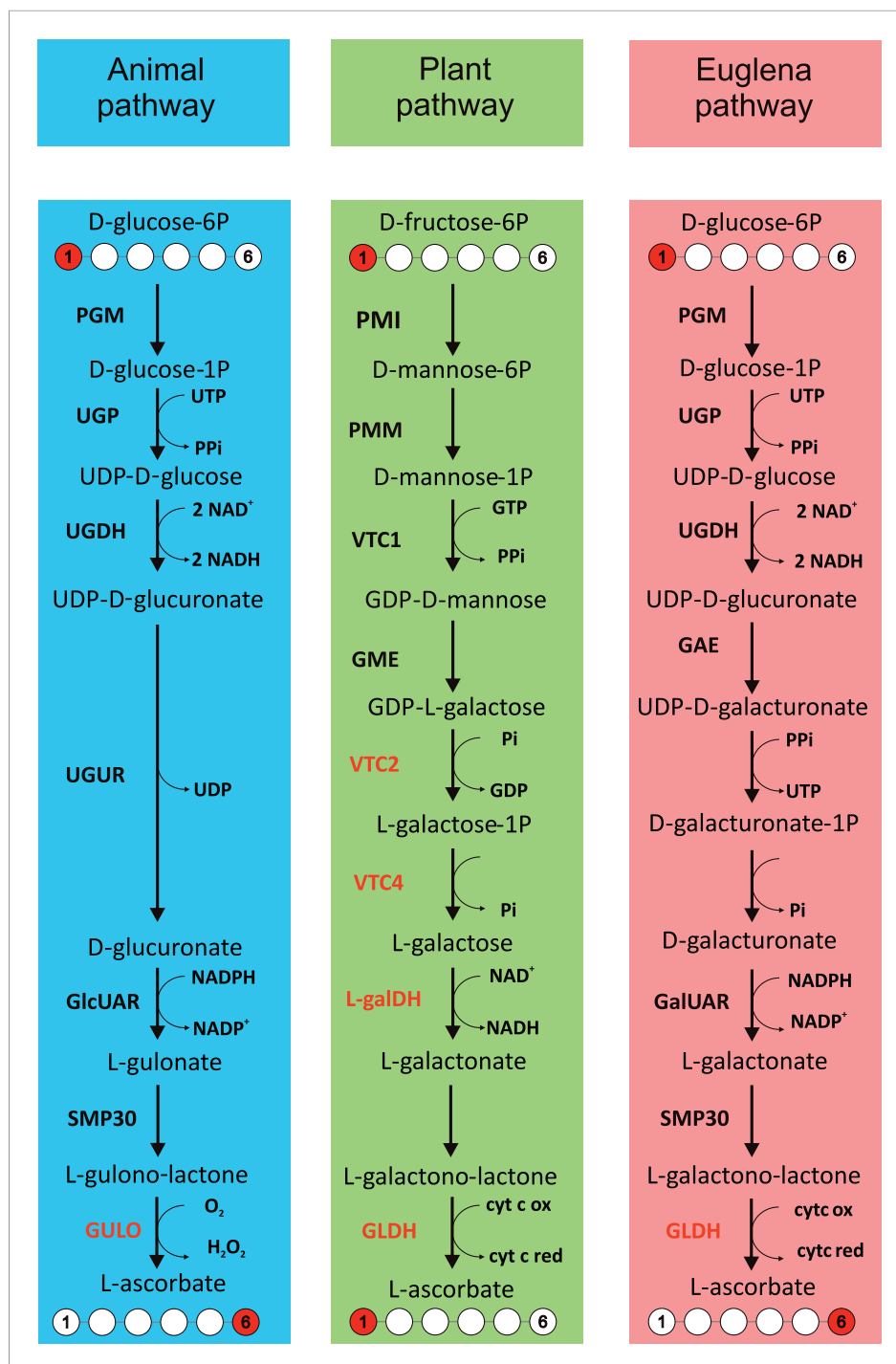
Glen Wheeler, et al.

Figure 1. Major ascorbate biosynthetic pathways in eukaryotes. The scheme depicts the three major ascorbate biosynthetic pathways found in eukaryotes (*Shigeoka et al., 1979*; *Wheeler et al., 1998*; *Linster and Van Schaftingen, 2007*). The plant pathway (also known as the Smirnoff-Wheeler or D-mannose/L-galactose pathway) involves no inversion of the carbon chain (i.e., C1 of D-glucose becomes C1 of L-ascorbate), whereas the euglenid and animal pathways involve inversion of the carbon chain in the conversion from uronic acid to aldonolactone (i.e., C1 of D-glucose becomes C6 of L-ascorbate). Our analyses focus on enzymes with a dedicated role in ascorbate biosynthesis (shown in red): GULO—L-GulL oxidase; VTC2—GDP-L-galactose phosphorylase; VTC4—L-galactose-1-phosphate phosphatase; L-galDH—L-galactose dehydrogenase; GLDH—L-GalL dehydrogenase. The other enzymes are: PGM—phosphoglucomutase; UGP—UDP-D-glucose pyrophosphorylase; UGDH—UDP-D-glucose dehydroge-nase; UGUR—UDP-glucuronidase; GlcUAR—D-glucuronate reductase; SMP30—regucalcin/lactonase; GAE—UDP-D-

Figure 1. continued on next page

Figure 1. Continued

glucuronate-4-epimerase; GalUAR—D-galacturonate reductase. Enzyme names are not listed for steps where multiple enzymes may be involved or where specific enzymes have not been identified.
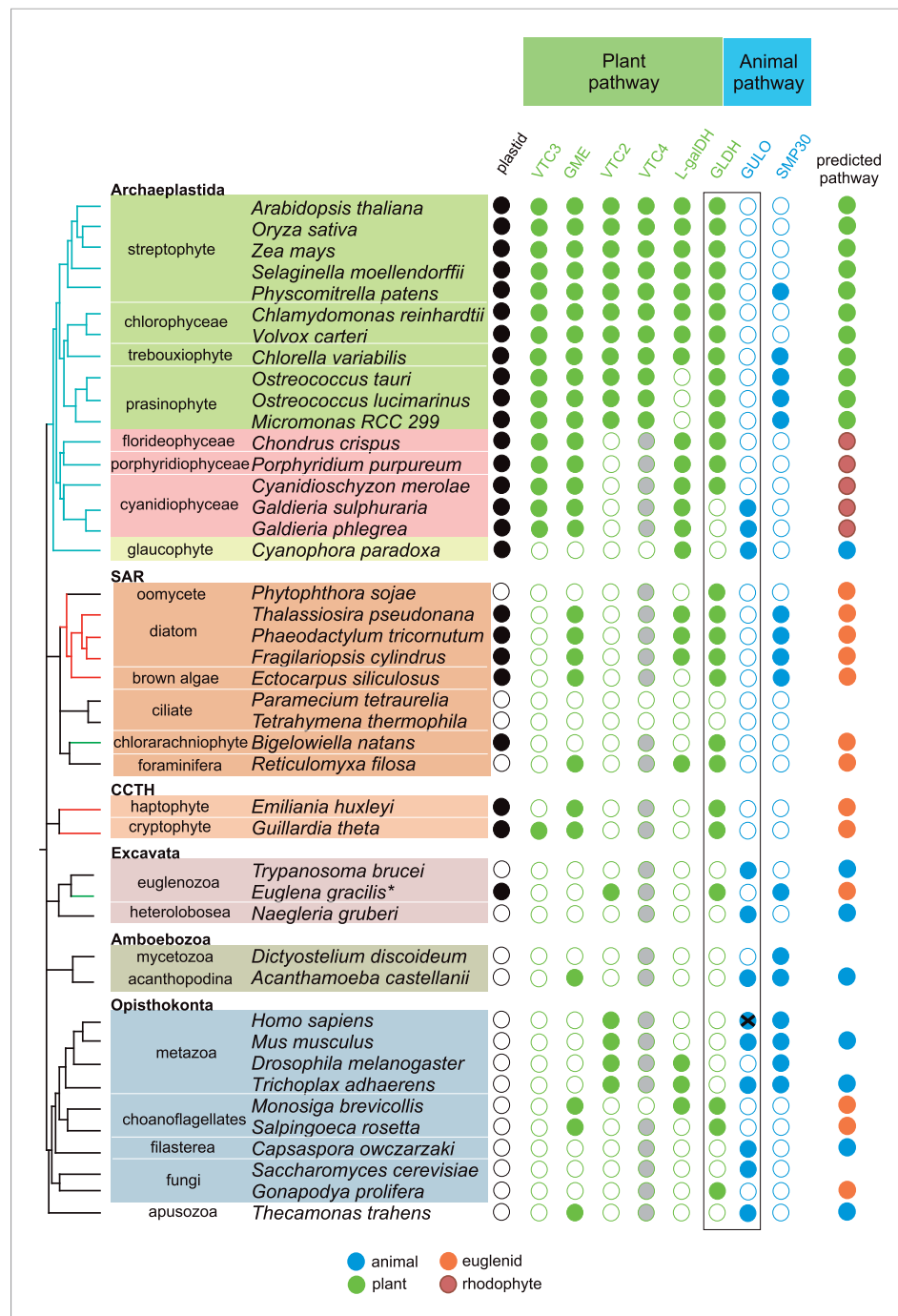DOI: 10.7554/eLife.06369.003

Figure 2. Coulson plot indicating the taxonomic distribution of the different ascorbate pathways. 40 eukaryote genomes were analysed for the presence of genes in the ascorbate biosynthetic pathways. The two potential terminal enzymes in the pathway are boxed. *GLDH* is common to both the 'plant' and 'euglenid' type pathways. A schematic tree depicts the currently accepted phylogenetic relationships between organisms. The predicted route of ascorbate biosynthesis in each organism is shown. Note that 'euglenid' and 'rhodophyte' type pathways cannot currently be distinguished from sequence analysis alone and the predictions are based on biochemical evidence. Asterisk denotes a genome assembly was not available for *Euglena gracilis* and its transcriptome was analysed ('Materials and methods'). Grey circles in VTC4 represent the presence of a highly similar enzyme, *myo*-inositol-1-phosphate phosphatase that exhibits l-galactose-1-phosphatase activity. GULO in trypanosomes and yeasts acts to oxidise the alternative substrates L-galactonolactone or D-arabinonolactone respectively. VTC3 is not a biosynthetic enzyme, but represents a dual function Ser/Thr protein kinase/protein phosphatase 2C that may play a regulatory role in the plant pathway (*Conklin et al., 2013*). Black cross represents a pseudogene encoding a non-functional

Figure 2. Continued

enzyme. Organisms with sequenced genomes that were found to lack both of the terminal enzymes in the known pathways (GULO and GLDH) are likely to be ascorbate auxotrophs and were not included in the plot. These include *Giardia intestinalis, Trichomonas vaginalis, Entamoeba invadens, Plasmodium falciparum* and *Perkinsus marinus*.
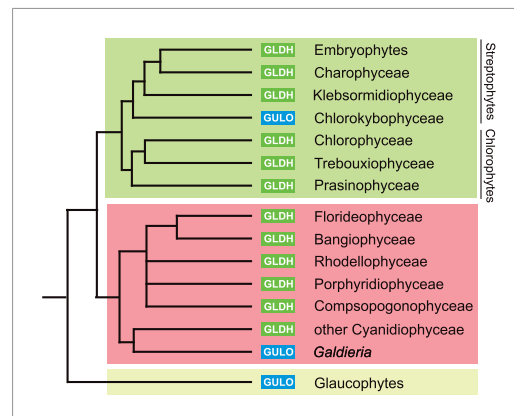
Figure 2—figure supplement 1. Distribution of GULO and GLDH in the Archaeplastida. A schematic tree demonstrating the currently accepted phylogenetic positions of the major lineages in the Archaeplastida (*Yoon et al., 2006*; *Leliaert et al., 2012*). The presence of either *GULO* or *GLDH* in representatives of each lineage is shown. The boxes denote the Viridiplantae (green), Rhodophyta (red) and Glaucophyta.
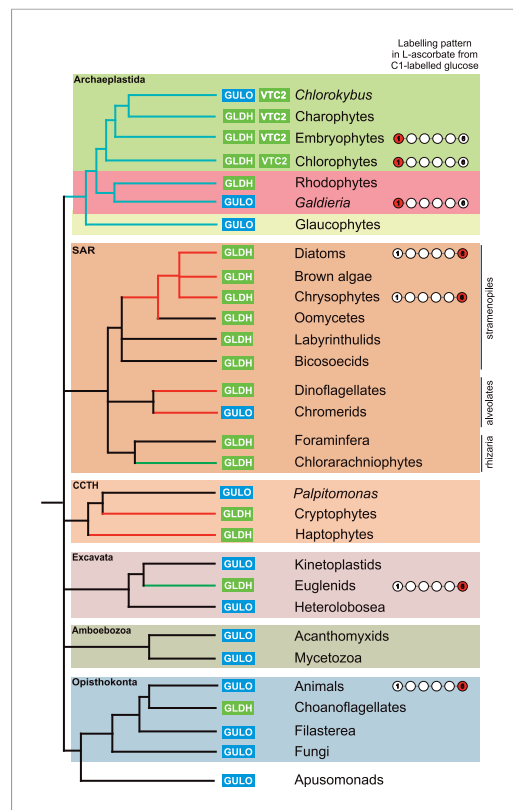
Figure 2—figure supplement 2. Distribution of the different ascorbate pathways. The schematic tree summarises the distribution of the two terminal enzymes in ascorbate biosynthesis, along with VTC2, the first committed enzyme in plant pathway. Blue lines indicate photosynthetic lineages derived by the primary endosymbiosis (of a cyanobacterium). Red or green lines indicate lineages that have become photosynthetic following a secondary endosymbiosis event with either a red or a green alga respectively. It should be noted that the timing and origin of many secondary endosymbioses remain unclear, particularly within the SAR supergroup where several non-photosynthetic lineages within the stramenopiles, alveolates and even rhizaria may potentially have lost an ancestral plastid. *GULO* is found in basally derived lineages of the Archaeplastida, Excavata, Opisthokonta, Amoebozoa and the CCTH group. In contrast, *GLDH* is found predominately in photosynthetic eukaryotes, although it is also found in non-photosynthetic stramenopiles and rhizaria and also in some choanoflagellates. Lineages where there is biochemical evidence determining inversion or non-inversion of the carbon chain in the conversion from D-glucose to ascorbate are shown.
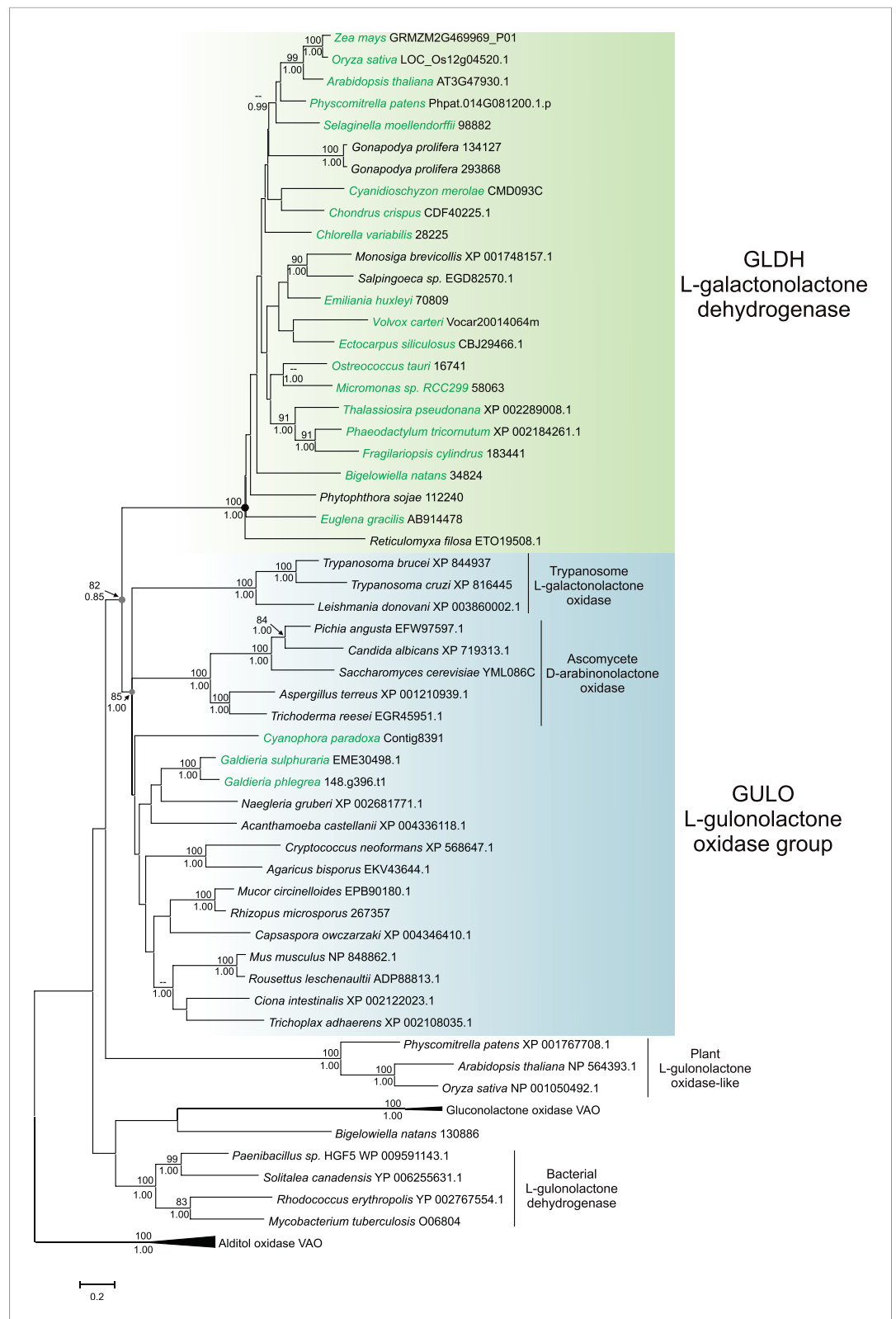DOI: 10.7554/eLife.06369.006

Figure 3. Phylogenetic analysis of ʟ-gulonolactone oxidase and ʟ-galactonolactone dehydrogenase. A maximum likelihood phylogenetic tree demonstrating the relationships between aldonolactone oxidoreductases involved in ascorbate biosynthesis. A multiple sequence alignment of 263 amino acid residues was used with alditol oxidases from the vanillyl alcohol oxidase (VAO) family acting as the outgroup. Photosynthetic organisms are shown in green. *Figure 3. continued on next page*

Figure 3. Continued

There is strong support for a monophyletic origin for *GLDH* in eukaryotes. Bootstrap values >80% are shown above nodes (100 bootstraps) and Bayesian posterior probabilities >0.95 are shown below (10000000 generations), except for selected key nodes (circled) where all values are displayed.

Figure 3—figure supplement 1. Phylogenetic analysis of L-galactonolactone dehydrogenase. An unrooted maximum likelihood phylogenetic tree of *GLDH*. To improve resolution of *GLDH* phylogeny, an individual phylogenetic analysis was performed using a larger alignment (302 amino acids) with greater taxonomic sampling (151 sequences), although relationships between major taxonomic groups remain poorly resolved. Bootstrap values >70% are shown (100 bootstraps).
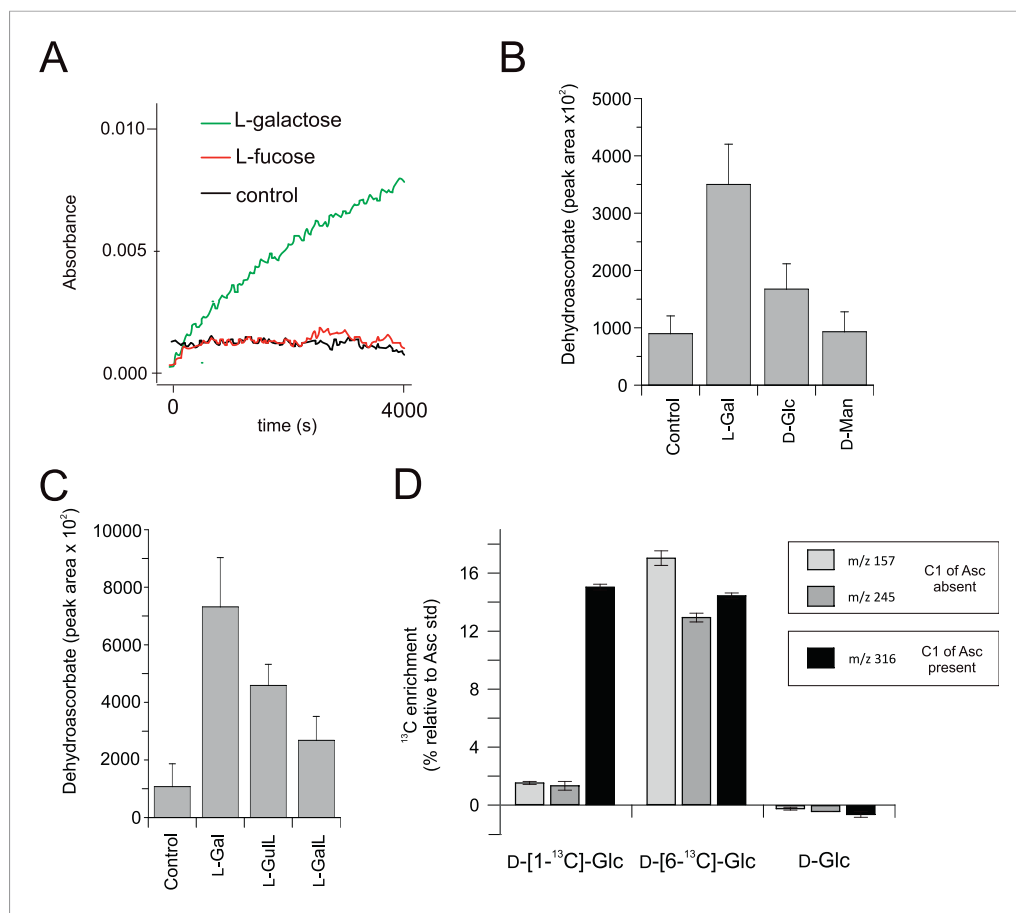
DOI: 10.7554/eLife.06369.008

Figure 4. Biochemical evidence for a modified D-mannose/L-galactose pathway in rhodophytes. (**A**) Crude extracts of *Porphyra umbilicalis* thallus demonstrate L-galactose dehydrogenase activity using 5 mM L-galactose (L-Gal) as a substrate. No activity was demonstrated with 5 mM L-fucose (6-deoxy-L-galactose) as a substrate. The result is representative of three different enzyme preparations. (**B**) Feeding 10 mM L-Gal to *Porphyra* thallus for 24 hr resulted in an accumulation of ascorbate (detected as dehydroascorbate—DHA). D-mannose (10 mM) did not cause an increase in ascorbate in *Porphyra*, but exogenous D-mannose does not elevate ascorbate in land plants even though it is an intermediate in ascorbate biosynthesis. The bar chart shows mean peak areas of selected fragments (±s.d.). n = 3. (**C**) Feeding ascorbate precursors (25 mM) to *Galdieria sulphararia* from both the plant and animal pathways results in increased cellular ascorbate (detected as dehydroascorbate using GC-MS) (±s.d.). The extent of the increase in cellular ascorbate is influenced by the rate of conversion of the intermediate and the rate of its uptake into the cell. n = 3. (**D**) Feeding D-[1-^{13}C]-glucose (25 mM) to *Galdieria sulphararia* results in enrichment of ^{13}C in the 316/317 m/z fragment of dehydroascorbate (which includes C1), but not in the 245/246 m/z or 157/158 m/z fragment (which exclude C1) (±s.d.). In contrast, feeding D-[6-^{13}C]-glucose (25 mM) labels all fragments, suggesting that they all include C6. In combination, this labelling pattern indicates plant-like non-inversion of the carbon chain in the conversion of hexoses to ascorbate. n = 3.
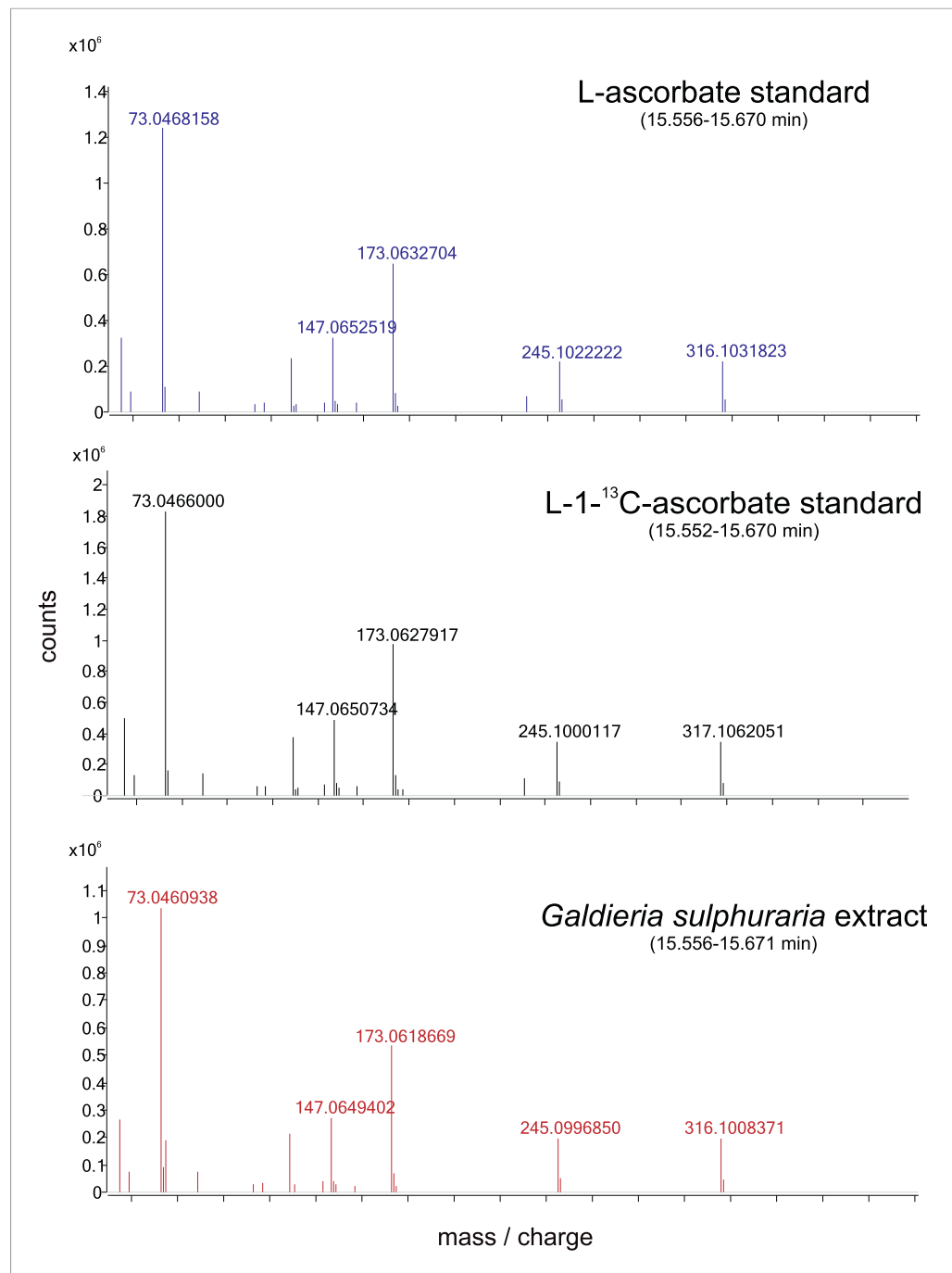DOI: 10.7554/eLife.06369.009

Figure 4—figure supplement 1. Positional isotopic labelling of ascorbate biosynthesis. Analysis of ascorbate by GC-MS. Ascorbate is oxidised to dehydroascorbate during the derivatisation process and representative accurate mass spectra are shown. Analysis of a L-[1-^{13}C]-ascorbate standard indicates that the m/z 316 fragment of dehydroascorbate contains C1 whilst other fragments (m/z 157 and 245) do not. Dehydroascorbate from *G. sulphuraria* extracts exhibits an identical retention time and mass spectra to that of the ascorbate standard.
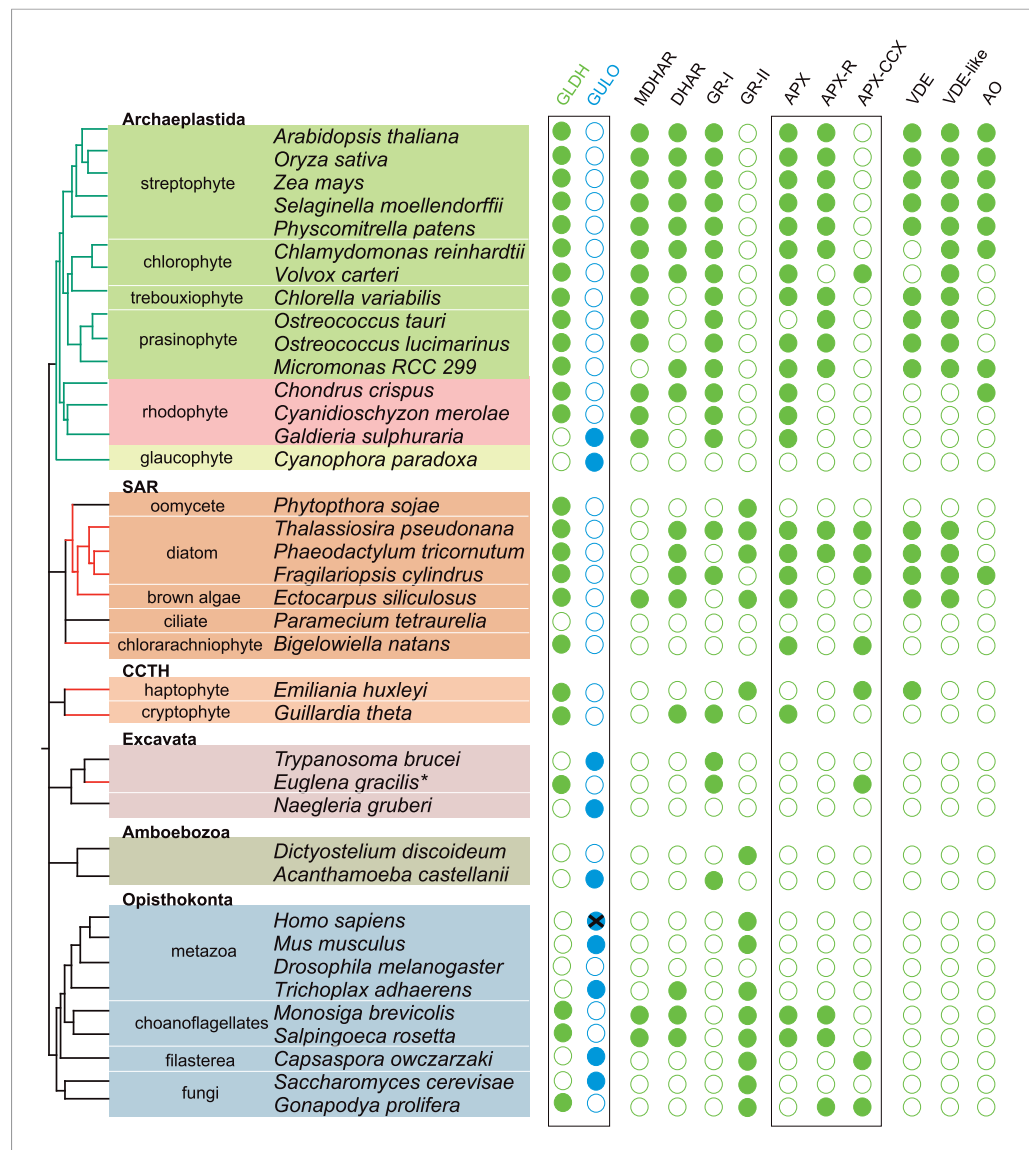DOI: 10.7554/eLife.06369.010

Figure 5. Coulson plot showing the distribution of photoprotective ascorbate-dependent enzymes. Eukaryote genomes were analysed for the presence of enzymes from the plant ascorbate-glutathione cycle, the xanthophyll cycle and other ascorbate-dependent enzymes. We found that eukaryotes possess two distinct isoforms of GSH reductase. PeroxiBase was used to distinguish between the different forms of ascorbate peroxidase (*Fawal et al., 2013*). Boxes highlight the terminal enzymes in the biosynthetic pathway and the ascorbate peroxidase family (APX, APX-R and APX-CCX). MDHAR—monodehydroascorbate reductase; DHAR—dehydroascorbate reductase; GR-I—glutathione reductase isoform I; GR-II—glutathione reductase isoform II; APX—ascorbate peroxidase; APX-R—ascorbate peroxidase-related; APX-CCX—hybrid ascorbate peroxidase/cytochrome c peroxidase; VDE—violaxanthin de-epoxidase; VDE-like—violaxanthin de-epoxidase like; AO—ascorbate oxidase.
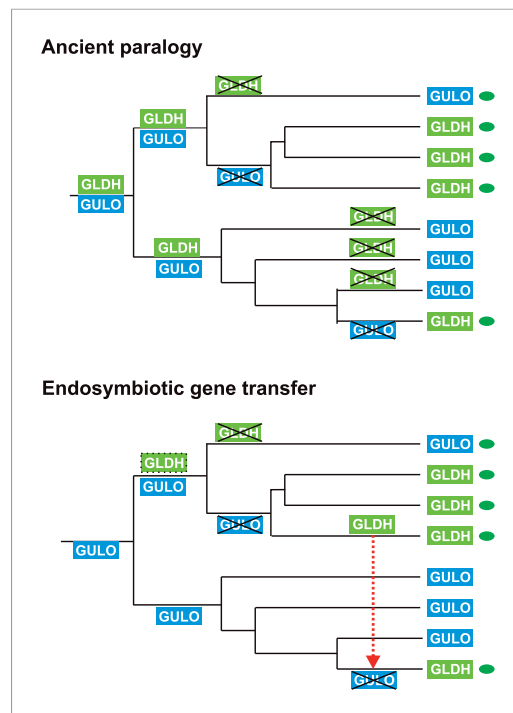DOI: 10.7554/eLife.06369.011

Figure 6. Evolutionary scenarios for *GULO* and *GLDH*. The scheme illustrates two most likely evolutionary scenarios responsible for the distribution of *GULO* and *GLDH* in eukaryotes. In the ancient paralogy scenario, an ancient gene duplication in the last common eukaryote ancestor results in the presence of two functionally similar genes, *GULO* and *GLDH*, followed by differential loss of either gene in each lineage. In the endosymbiotic gene transfer (EGT) scenario, *GULO* represents the ancestral gene and *GLDH* represents a novel gene that arose in a specific lineage. EGT of *GLDH* (red dashed arrow) to other photosynthetic lineages (green ovals) enables functional replacement of the ancestral gene. Note that *GULO* represents an ancestral gene in both of these evolutionary scenarios.
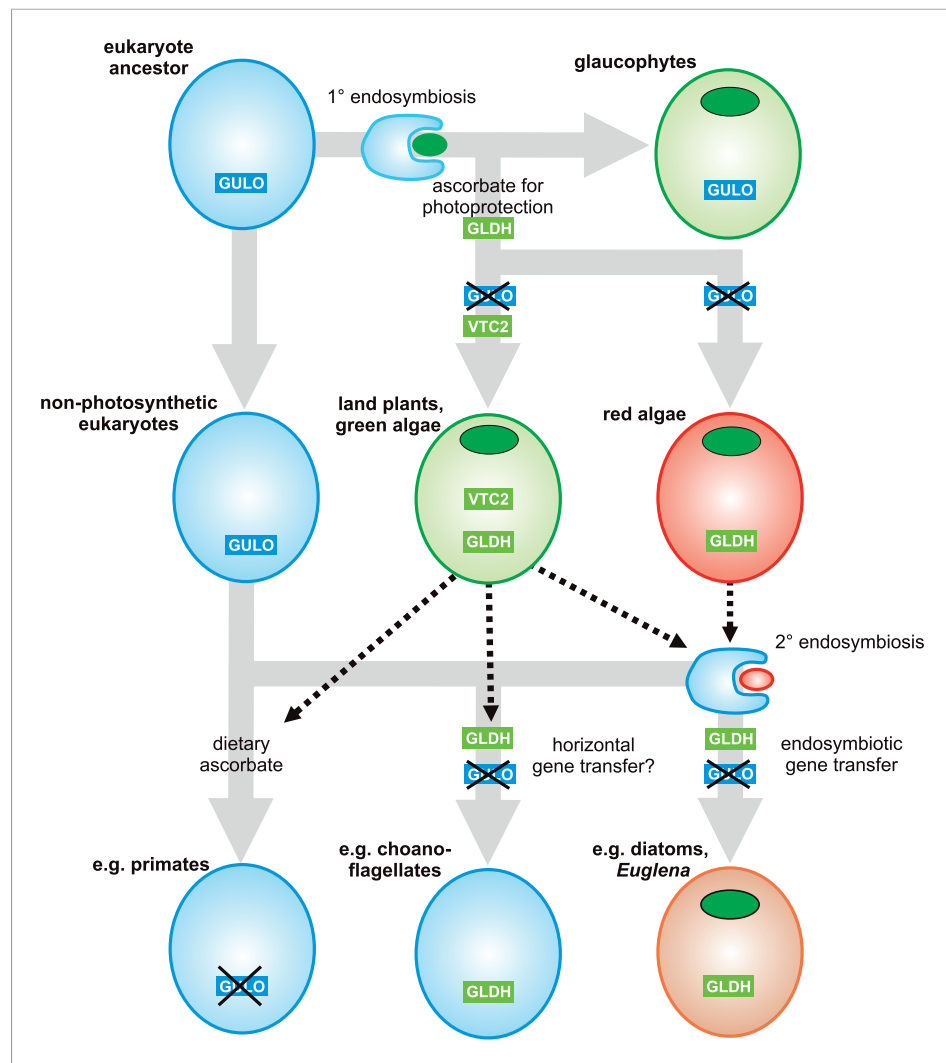DOI: 10.7554/eLife.06369.012

Figure 7. A proposed evolutionary model of ascorbate biosynthesis. The scheme illustrates the proposed events in the EGT evolutionary model of eukaryote ascorbate biosynthesis. In this scenario, ancestral eukaryotes synthesised ascorbate via GULO. *GLDH* arose in the Archaeplastida following primary endosymbiosis of a cyanobacterium, after the divergence of the glaucophyte lineage. *GLDH* functionally replaced *GULO* in the red and green algal lineages, coinciding with the rise of the photoprotective role of ascorbate. Plastid acquisition via secondary endosymbiosis of either a green or red alga resulted in endosymbiotic gene transfer of *GLDH* and replacement of *GULO*. As these organisms became the dominant primary producers in many ecosystems, a series of trophic interactions (dotted lines) resulted in the loss of *GULO* in non-photosynthetic organisms, either by providing a ready supply of dietary ascorbate (resulting in ascorbate auxotrophy in heterotrophic organisms) or through putative horizontal gene transfer of *GLDH* (e.g., choanoflagellates). For clarity, not all potential trophic interactions are shown.
DOI: 10.7554/eLife.06369.013